ISOABE 99-7215

Propulsion System Airframe Integration Issues and Aerodynamic Database Development for the Hyper-X Flight Research Vehicle

Walter C. Engelund,
Scott D. Holland,
Charles E. Cockrell, Jr.
NASA Langley Research Center, Hampton, VA
and
Robert D. Bittner
FDC-NYMA, Inc., Hampton, VA

XIV ISOABE
September 5-10, 1999
Florence, Italy

PROPULSION SYSTEM AIRFRAME INTEGRATION ISSUES AND AERODYNAMIC DATABASE DEVELOPMENT FOR THE HYPER-X FLIGHT RESEARCH VEHICLE

Walter C. Engelund,[*] Scott D. Holland,[**] Charles E. Cockrell, Jr.[†]
NASA Langley Research Center, Hampton, VA
and
Robert D. Bittner[‡]
FDC-NYMA, Inc., Hampton, VA

Abstract

NASA's Hyper-X Research Vehicle will provide a unique opportunity to obtain data on an operational airframe integrated scramjet propulsion system at true flight conditions. The airframe integrated nature of the scramjet engine with the Hyper-X vehicle results in a strong coupling effect between the propulsion system operation and the airframe's basic aerodynamic characteristics. Comments on general airframe integrated scramjet propulsion system effects on vehicle aerodynamic performance, stability, and control are provided, followed by examples specific to the Hyper-X research vehicle. An overview is provided of the current activities associated with the development of the Hyper-X aerodynamic database, including wind tunnel test activities and parallel CFD analysis efforts. A brief summary of the Hyper-X aerodynamic characteristics is provided, including the direct and indirect effects of the airframe integrated scramjet propulsion system operation on the basic airframe stability and control characteristics.

Nomenclature

α angle-of-attack (degrees)

β angle-of-sideslip (degrees)

b_{ref} Hyper-X vehicle reference span

C_D Drag force coefficient ($\frac{drag}{q_\infty S_{ref}}$)

---

[*]*Aerospace Engineer, Vehicle Analysis Branch.*
[**]*Assistant Branch Head, Aerothermodynamics Branch.*
[†]*Aerospace Engineer, Hypersonic Airbreathing Propulsion Branch.*
[‡]*Section Supervisor, Hypersonic Numerical Applications Section.*

C_L Lift force coefficient ($\frac{lift}{q_\infty S_{ref}}$)

C_l Rolling moment coefficient ($\frac{rolling\ moment}{q_\infty S_{ref} b_{ref}}$)

$C_{l_{\delta a}}$ Rolling moment coefficient derivative due to aileron deflection (per degree)

C_{l_β} Rolling moment coefficient derivative with respect to sideslip angle

C_m Pitching moment coefficient ($\frac{pitching\ moment}{q_\infty S_{ref} l_{ref}}$)

C_n Yawing moment coefficient ($\frac{yawing\ moment}{q_\infty S_{ref} b_{ref}}$)

C_{n_β} Yawing moment coefficient derivative with respect to sideslip angle

$C_{n_{\delta a}}$ Yawing moment coefficient derivative due to aileron deflection (per degree)

C_Y Side force coefficient ($\frac{side\ force}{q_\infty S_{ref}}$)

C_{Y_β} Side force coefficient derivative with respect to sideslip angle

$C_{Y_{\delta a}}$ Side force coefficient derivative due to aileron deflection (per degree)

δ_a aileron deflection (differential horizontal tail: $\delta_{rw} - \delta_{lw}$), degrees

δ_{elv} elevon deflection (symmetric horizontal tail: $\frac{\delta_{rw} + \delta_{lw}}{2}$), degrees

δ_r rudder deflection ($\frac{\delta_{rr} + \delta_{lr}}{2}$), degrees

l_{ref} Hyper-X vehicle reference length

q_∞ freestream dynamic pressure ($\frac{1}{2}\rho_\infty V_\infty^2$)

S_{ref} Hyper-X vehicle reference area

Introduction

The primary goals of NASA's Hyper-X program are to demonstrate and validate the technologies, the experimental techniques, and the computational methods and tools required to design and develop hypersonic aircraft with airframe-integrated dual-mode scramjet propulsion systems. Three Hyper-X vehicles, the first two of which will fly at Mach 7, and the third at Mach 10, will provide the first ever opportunity to obtain data on airframe integrated scramjet propulsion systems at true flight conditions.[1-3] For vehicles such as Hyper-X, where the distinct lines between the airframe and the propulsion system are blurred, there exists a very high degree of coupling between the airframe aerodynamics and the propulsion system's basic operation and performance characteristics. Even at this point in the Hyper-X program prior to first flight, a tremendous amount of knowledge has been gained through ground test and CFD analysis efforts regarding the scramjet propulsion system and airframe aerodynamic interactions. The primary objective of the three Hyper-X flight tests is to obtain data on the operating characteristics and performance of a dual mode scramjet propulsion engine system. In addition, an extensive amount of data will be obtained on the vehicle's basic aerodynamic characteristics, both during the period of scramjet engine operation and after the actual engine test has been completed. The Hyper-X flight research vehicles will provide an extensive set of research quality flight data at hypersonic conditions for a slender body airframe with an integrated scramjet propulsion system. Each of the three Hyper-X flight vehicles will be heavily instrumented with over 100 individual surface pressure transducers and thermocouples, and a high-resolution three-axis accelerometer package. An extensive amount of surface pressure and temperature data will be collected so that direct comparisons can be made with the preflight wind tunnel and CFD database. These pressure and temperature measurements will also be heavily utilized in the post-flight trajectory reconstruction efforts, which will aid in the determination of the actual atmospheric flight conditions over the entire flight test.

Hyper-X Vehicle Design and Mission Profile Description

The Hyper-X Research Vehicle (HXRV) design draws heavily on past vehicle configuration studies including the extensive U.S. National Aero-Space Plane (NASP) design database and several of the more recent U.S. hypersonic vehicle mission studies.[4,5] The three HXRVs are each 12 feet long, weight approximately 3000 lb, and are scramjet powered, lifting body configurations,
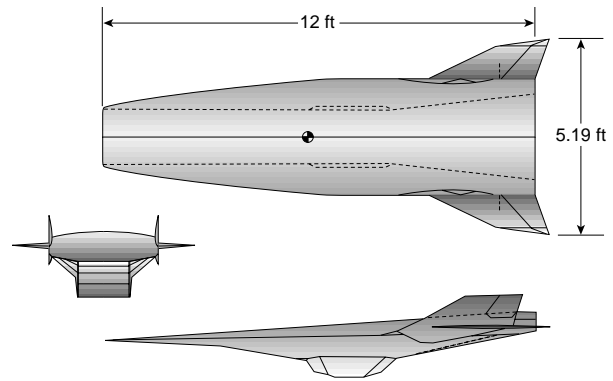
Figure 1. Hyper-X Research Vehicle (HXRV) configuration.

with all moving horizontal tails and twin vertical tails with rudder surfaces (Fig. 1). The scramjet flowpath, which begins at the nose of the vehicles, utilizes the entire underside of the forebody as a compression surface. The engine combustor is located on the vehicle undersurface, slightly aft of midbody, and the aftbody undersurface comprises the external expansion surface for the scramjet exhaust flow.

The nominal Hyper-X flight trajectories each begin with a boost to the scramjet engine test conditions on a modified version of an Orbital Sciences Corporation Pegasus® Hybrid rocket, referred to as the Hyper-X Launch Vehicle or HXLV. The HXLV is carried aloft under the wing of NASA's B-52 aircraft where, in the case of the first two Mach 7 experiments, it is dropped at an altitude of approximately 20,000 ft and a Mach number of 0.5. Shortly after drop, the booster solid rocket motor is ignited and the HXLV flies a nominal ascent profile to the HXRV test point as indicated in Fig. 2. At a point just prior to the scramjet engine test, the Hyper-X flight vehicle is separated from the launch vehicle.

Immediately following the stage separation event, the HXRV control system stabilizes the vehicle and the scramjet test portion of the experiment will begin. The scramjet engine inlet door will be opened, and the scramjet fueling sequence will commence. A combination of Silane (SiH_4) and gaseous hydrogen (H_2) is injected into the combustor region, resulting in powered scramjet engine operation. Silane is used only during the initial ignition process, after which pure hydrogen is injected and combusted. After the fuel is depleted, the flight vehicle will record several seconds of engine-off aerodynamic tare data, and conduct a brief series of aerodynamic parameter identification maneuvers. These maneuvers will allow the basic aerodynamic stability and control characteristics of the airframe to be estimated from the flight
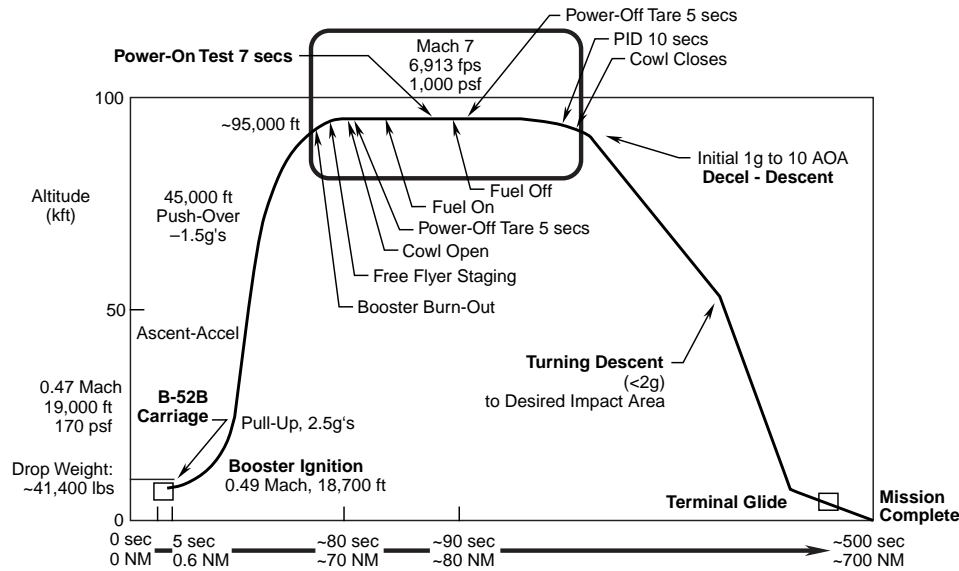
Power-Off Tare 5 secs

Power-On Test 7 secs

Mach 7
6,913 fps
1,000 psf

PID 10 secs

Cowl Closes

Altitude
(kft)

100

~95,000 ft

45,000 ft
Push-Over
−1.5g's

Initial 1g to 10 AOA
Decel - Descent

Fuel Off

Fuel On

Power-Off Tare 5 secs

Cowl Open

Free Flyer Staging

Booster Burn-Out

50

Ascent-Accel

Turning Descent
(<2g)
to Desired Impact Area

0.47 Mach
19,000 ft
170 psf

**B-52B
Carriage**

Pull-Up, 2.5g's

Drop Weight:
~41,400 lbs

Booster Ignition
0.49 Mach, 18,700 ft

Terminal Glide

**Mission
Complete**

0

0 sec
0 NM

5 sec
0.6 NM

~80 sec
~70 NM

~90 sec
~80 NM

~500 sec
~700 NM

Figure 2. Nominal Mach 7 Hyper-X flight profile.

data, which will then be compared with the preflight estimates developed using the ground based wind tunnel testing and analytical and computational methods. Immediately following these maneuvers, the inlet cowl door will be shut and the vehicle will fly a controlled deceleration trajectory as it descends and decelerates through the supersonic and transonic flight regimes prior to flight termination at subsonic conditions.

Comments on Airframe Integrated Scramjet Propulsion System and Airframe Aerodynamic Interactions

A point that is absolutely crucial in the design and operation of the Hyper-X vehicles, and any future vehicle configurations that will utilize highly integrated scram/ramjet or combined cycle propulsion systems, is a complete understanding of the interactions between the propulsion system and the vehicle airframe aerodynamics. Propulsion system airframe integration issues must be taken into consideration early in the design process if overall vehicle performance goals are to be met. For vehicles such as Hyper-X, there exists a very high degree of coupling between the airframe aerodynamics and the propulsion system's basic operation and performance characteristics. Historically, the hypersonic airbreathing propulsion community has focused on engine thrust optimization with little effort devoted to the quantification of contributions to lift and/or pitching or yawing moments. From an overall vehicle design perspective, the importance of being able to predict and account for these "other" forces and moments can not be overstated.

In the past, external airframe design, including body contouring and lifting surface and control sizing (wings, tails, elevators, ailerons, etc.), could be accomplished somewhat independent of the propulsion system design and development process. Final design modifications could be accomplished after the airframe and propulsion systems had been matured to a relatively high degree, essentially independent of one another. However, for supersonic/hypersonic flight vehicles that will utilize propulsion systems which are highly integrated with the airframe (e.g. scramjets), the design and development process must take into account the interactions between the two now tightly coupled disciplines of propulsion and aerodynamics.

In order to develop the aerodynamics and propulsion databases for vehicle design, proper force accounting methods and strategies must be developed and agreed upon by the external airframe aerodynamics and the propulsion groups to ensure that forces and moments from all surfaces are properly accounted for. An example of the Hyper-X basic force accounting system is shown in Fig. 3.

In the case of the Hyper-X configuration, the vehicle aftbody serves as the nozzle expansion surface. This aftbody expansion surface, over which the high pressure scramjet exhaust gases are expanding, has a large corresponding moment arm relative to the vehicle center of gravity. This implies that variable engine thrust levels can have significant impact on the vehicle pitching moment and the corresponding control surface deflections required to aerodynamically trim the vehicle. If not prop-
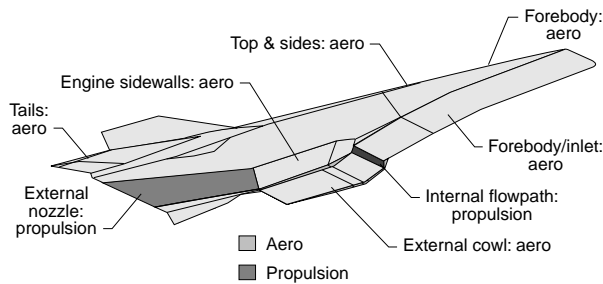
Figure 3. Hyper-X aerodynamic and propulsion force accounting system.

erly accounted for early in the design, the aerodynamic drag associated with large control surface trim deflections may become a substantial portion of the vehicle total drag and can adversely affect the ability of the vehicle to meet its mission requirements. In addition to the direct effects of engine operation on vehicle pitch and corresponding trim drag, control surface deflections required to trim the vehicle in the longitudinal plane may have a substantial effect on the vehicle's lateral-directional stability and control characteristics, thereby implying an indirect effect of the propulsion system operating conditions on the lateral-directional aerodynamic behavior. Since the Hyper-X vehicles are designed for scramjet operation at two distinct Mach numbers (7 and 10), this is only a concern at these specific discrete points. However, a vehicle with a similar airframe integrated propulsion system required to operate over a wide range of Mach numbers from subsonic through hypersonic cruise would require design considerations and allowances that would ensure optimal performance and acceptable airframe/propulsion aerodynamics over the entire flight envelop. Finally, care must be taken to ensure that the engine exhaust plume must not adversely affect the vehicle aerodynamic control surfaces in a manner that vehicle control is compromised.

Hyper-X Research Vehicle Aerodynamic Database Development Efforts

Because of the highly integrated nature of the scramjet engine with the HXRV airframe, an extensive combination of wind tunnel testing and CFD analysis has been required to determine the HXRV's aerodynamic characteristics. Early in the program, initial wind tunnel screening tests were conducted to determine the basic airframe aerodynamics, including stability, control, and performance characteristics. These quick assessment tests were conducted in the NASA Langley 20-inch Mach 6 and 31-inch Mach 10 facilities,[6] the Boeing – St. Louis Polysonic tunnel,[7] and the Boeing North American subsonic tunnel.[7] As the vehicle design matured, addi-

tional testing was conducted using larger (12.5%), higher fidelity models with higher resolution control surface increments. Additional entries using the high fidelity models have been made, and further tests are planned, in the Langley 20-inch Mach 6 and 31-inch Mach 10 tunnels. Information regarding specific details of several of the tests is provided in Ref. 8.

Due to the relatively small scale of the wind tunnel models, inlet-open testing (unpowered or powered using a simulant gas) was not possible. A comprehensive CFD study was undertaken to provide estimates of the inlet-open unpowered and powered flight aerodynamic characteristics for the Mach 7 vehicles[8,9] including the effects of Mach number, angle-of-attack and sideslip on the HXRV. CFD and analytical analysis methods have also been utilized to bridge the gap from wind tunnel to flight conditions. This includes accounting for issues associated with Reynolds number scaling, scramjet propulsion flowfield induced effects, force and moment increments associated with opening the inlet door, tunnel hardware interference, and unsteady flow effects. Current CFD efforts are also focused on the Mach 10 vehicle design and propulsion flowpath refinements utilizing a total vehicle closure approach.

Flight data will also be utilized to update and improve the Hyper-X aerodynamic database. Aerodynamic parameter identification maneuvers, which will be performed immediately following the scramjet engine test and at various points during the Hyper-X Research Vehicle's descent trajectory, will allow a maximum amount of aerodynamic stability and control data to be gleaned from the flight tests. The results of the flight derived data will then be fed back into the preflight aerodynamic models to complete the Hyper-X aerodynamic database, as indicated in Fig. 4.

The basic inlet open, unpowered and powered force and moment incremental predictions, derived initially from CFD analyses, are being verified experimentally by test-
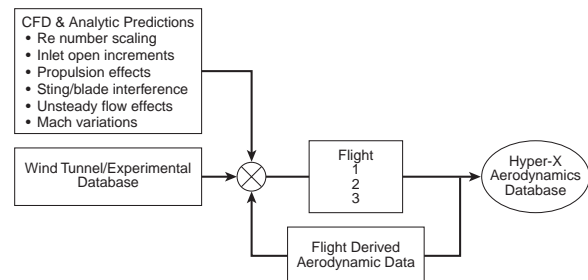

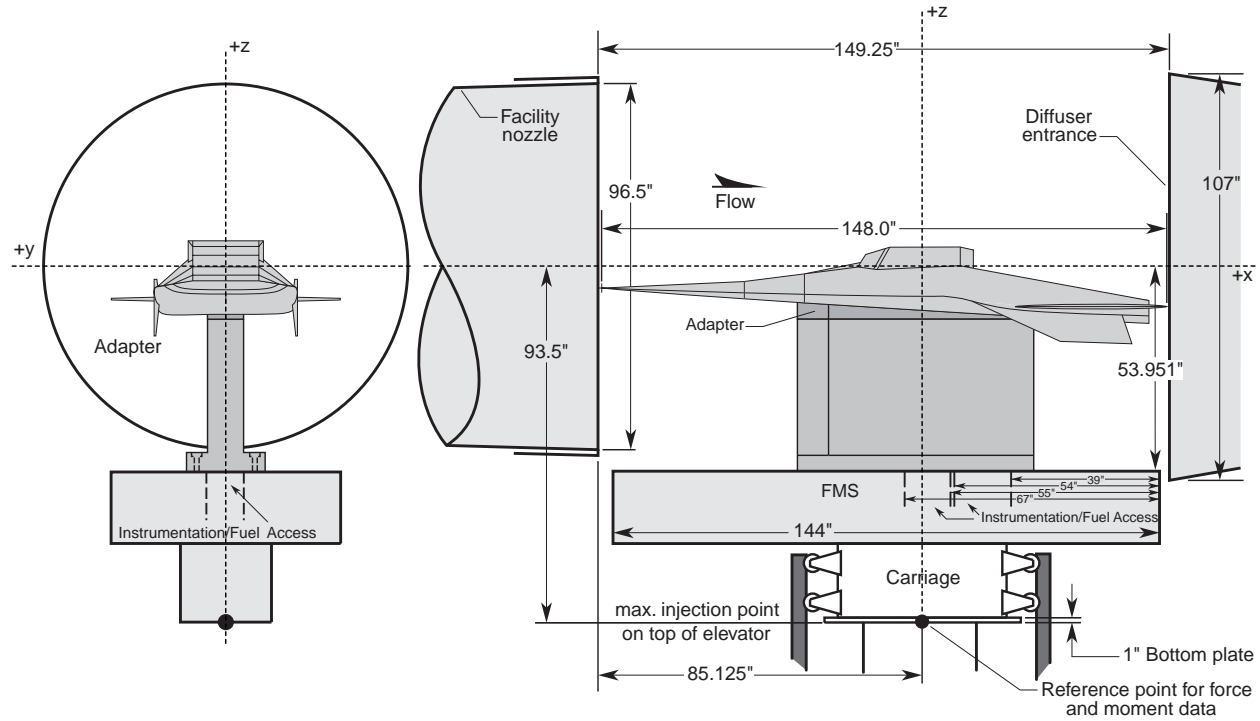*Figure 4. Hyper-X aerodynamic database development process.*

Figure 5. Diagram of the Hyper-X flight vehicle installation in the NASA Langley 8 ft HTT.

ing a full scale HXRV model in the NASA Langley 8-ft High Temperature Tunnel (8-ft HTT).[10] The 8-ft HTT facility provides the capability to test the full scale flight vehicle at flight conditions (Mach, pressure, and enthalpy). The primary intent of this test is to verify the propulsion system fuel sequencing and operation, validate the flight vehicle structural integrity, and to check the operational capabilities of various flight subsystems in a simulated flight environment. In addition, this test will provide the aerodynamic force and moment incremental data that will result from the cowl inlet opening and closing, and the fuel on (powered) portion of the flight. Additional CFD analysis efforts are focusing on the quantification of the effects of the 8-ft HTT vitiated air test gas vs. actual flight test conditions. The 8-ft HTT test will not provide overall vehicle force and moment data due to the fact that the full scale flight vehicle span extends beyond the tunnel core flow, as well as the aerodynamic interference effects associated with the large mounting strut that is required to support the model in the tunnel, as indicated in Fig. 5. However, the propulsion flowpath is well within the high quality core flow of the tunnel, so that the test should provide high quality data on the increments associated with the inlet door opening and closing and the propulsion power up transients. This data will aid in the benchmarking assessments of the computational predictions.

Results and Discussion

It is not within the scope of this brief overview paper to present the results from the entire Hyper-X vehicle aerodynamic database. Instead, some of the salient points and highlights of the HXRV aerodynamic characteristics at and around the scramjet engine test point are presented and discussed.

The basic longitudinal aerodynamic characteristics for the HXRV airframe (inlet door closed configuration) at Mach 6 conditions are shown in Fig. 6. The experimental results, obtained on the high fidelity 12.5% scale (18 inch) model in the most recent test entry in the NASA LaRC 20-inch Mach 6 wind tunnel, indicate well behaved, relatively linear lift characteristics over the anticipated flight angle-of-attack and elevator deflection angle range. Drag coefficient data are also shown as a function of angle-of-attack and elevator deflection angle. The pitching moment coefficient data, shown here as a function of angle-of-attack for elevator deflection angles of 0, 7.5 and 15 degrees, indicate an airframe with positive longitudinal stability (negative C_{m_α} slope) up to angles-of-attack of approximately eight degrees. At angles-of-attack beyond eight degrees the configuration becomes neutrally stable. An elevator deflection angle of approximately seven degrees is required to trim the vehicle at the Mach 6 nominal two degrees angle-of-
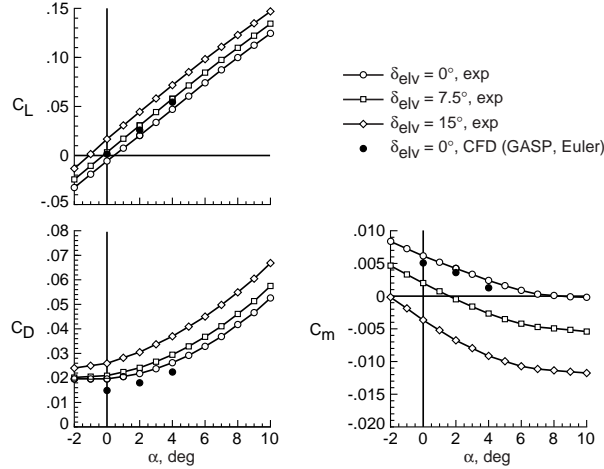
Figure 6. HXRV Mach 6 basic longitudinal aerodynamic characteristics (wind tunnel and CFD results).

Figure 8. Effects of the sting and blade mount interference on the HXRV Mach 6 basic longitudinal characteristics.

attack for the inlet closed configuration data shown here. Results from a series of inviscid CFD solutions obtained at Mach 6 conditions at each of zero, two, and four degrees angle-of attack, all with zero degree elevon deflection, are also included on the plots of Fig. 6. The CFD predicted results for the lift and pitching moment values agree relatively well with the wind tunnel data, while the discrepancies in the CFD drag predictions are due primarily to the fact that they were obtained from a inviscid analysis; the higher drag coefficient data obtained in the wind tunnel is directly attributable to the viscous (skin friction) effects.

During this same wind tunnel test entry, the HXRV model was mounted with a blade strut balance and tested in the presence of a removable, non-metric, false sting, such that sting interference effects could be directly computed. A similar non-metric false blade strut was utilized with the standard sting mount model to compute the corresponding strut interference effects (Fig. 7).
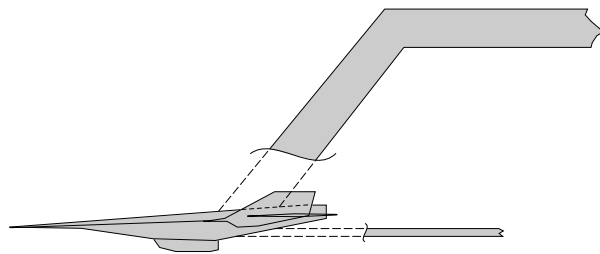

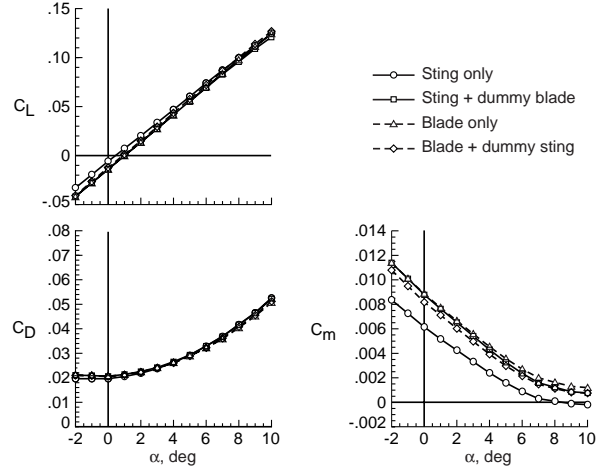*Figure 7. Sting and blade mount adapter hardware for the HXRV wind tunnel tests.*

An example of the results of this series of tests are shown in Fig. 8, in which the lift, drag, and pitching moment data are shown for the HXRV configuration with the sting only, blade only, sting + false blade, and a blade + false sting arrangement. Close inspection of this figure reveals the fact that the effect of the blade mount is rather dramatic in pitching moment, and to a lesser degree in the lift and drag coefficient data. From this series of tests, a set of increments were derived to account for the sting mount interference by taking the differences of the blade mount + false sting and the blade mount alone data.

The basic longitudinal effects of opening the inlet door and of scramjet powered operation at the Mach 7 test conditions are indicated in Fig. 9. Basic pitching moment data are shown for the zero degree elevon deflection, inlet door closed configuration. This data was derived from the Mach 6 wind tunnel test data and a set of CFD derived increments, which account for the Mach 6 to Mach 7 condition scaling. CFD analysis was also utilized to develop the force and moment increments associated with opening the inlet door and with the scramjet powered engine operation. Inspection of the basic pitching moment data indicates that a slight nose down moment increment is expected as a result of opening the inlet door. The inlet door, in the closed position, can be viewed as a third forebody compression ramp. The high pressure acting over this surface, which is located well below and slightly aft of the vehicle c.g., acts to pitch the vehicle down. By opening the door, the compression angle is effectively reduced, as is the ramp orientation relative to the c.g., which results in a nose up pitching moment associated with this surface motion. However, by opening the inlet door, flow thru conditions are es-
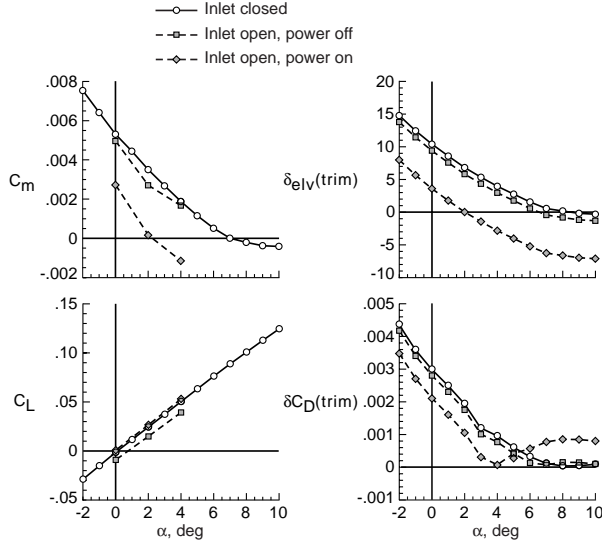
Figure 9. Comparison of the HXRV inlet closed and inlet open, unpowered and powered basic longitudinal characteristics.

tablished and the aftbody nozzle expansion surface is pressurized, which tends to nose the vehicle down. These two opposing effects tend to cancel each other, and the net result is a slight nose down pitch increment. The increment requires approximately 6 degrees of elevon deflection to trim at the nominal two degree angle-of-attack test condition (vs. the 7 degree deflection required for inlet closed operation at Mach 7). At the same time, the act of opening the inlet door results in a substantial loss of lift on the vehicle. This is due primarily to the loss of the contribution to lift of the pressure forces acting normal to the inlet door in its closed position.

In the nominal scramjet powered operation mode (inlet open, power-on data of Fig. 9), there is a substantial nose down pitching moment increment, which has been estimated using an additional set of CFD analyses. In this case, two opposing sets of forces act to produce a net nose down moment increment. The momentum flux exiting the scramjet engine combustor (located below the vehicle c.g.) produces a slight nose up moment; this, however, is small in comparison to the nose down moment increment that results from the aftbody nozzle surface area of the vehicle being pressurized by the expanding scramjet exhaust flow. In addition to the net nose down moment increment, nominal scramjet operation provides a substantial increment in overall lift, as a result of the high pressure scramjet exhaust flow acting over the nozzle aftbody. Because of the large nose down moment increment, the required elevon deflection angle to trim the configuration at two degrees angle-of-attack is effectively reduced to zero. This is advantageous from

a vehicle performance point of view because of the fact that large trim drag penalties are associated with the elevon surface deflections. The increments to vehicle drag coefficient associated with trimming the vehicle over the angle-of-attack (alpha) range from –2 to +10 degrees are also indicated in Fig 10 for each of the inlet closed, inlet open/power-off, and inlet open/power-on conditions. Trimmed flight at the nominal Mach 7, 2 degree angle-of-attack test condition with the inlet closed requires approximately 7 degrees of elevon deflection. This results in a trim drag coefficient penalty of roughly 0.020, which is approximately 11% of the basic untrimmed inlet closed configuration vehicle drag. During nominal scramjet engine operation the trim drag penalty is greatly reduced, which should maximize the vehicle performance margin. This issue of aerodynamic trim drag is a key design consideration which must be taken into account for future hypersonic vehicles that will utilize airframe integrated propulsion systems.

Substantial efforts have been made to assess the effects of inlet open unpowered and powered operation on the basic lateral-directional characteristics of the HXRV airframe as well. The wind tunnel tests provided data for only the inlet closed configuration (due to model and wind tunnel scale limitations, inlet-open flow thru and powered simulation testing was not possible). The basic airframe lateral-directional characteristics at Mach 7 are shown in Fig. 10. The inlet closed results, derived from wind tunnel tests in the LaRC 20-inch Mach 6 and 31-in Mach 10 facilities, indicate a directionally stable vehicle (positive values of C_{n_β}) over the anticipated flight angle-of-attack range. The configuration also has posi-
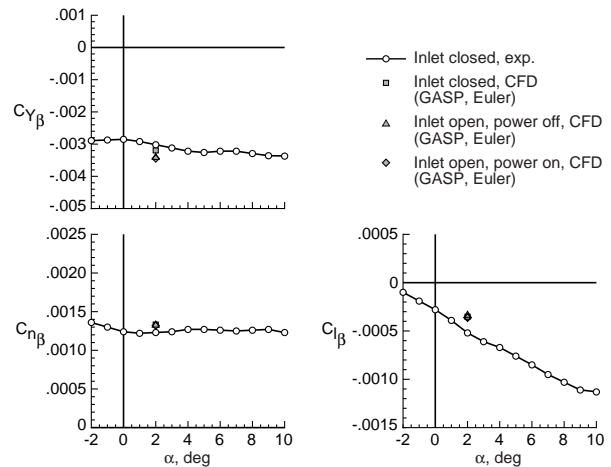

Figure 10. Comparison of the HXRV inlet closed and inlet open, unpowered and powered basic lateral-directional characteristics (wind tunnel and CFD data)

7

tive roll stability or effective dihedral (negative values of C_{l_β}) and a nearly constant induced side force at sideslip (β) conditions. Once again, in order to address the issue of inlet open unpowered and powered operation, CFD analyses were conducted on the configuration at sideslip conditions.[9] At issue was the question of the effect of vehicle sideslip and the expanding propulsion plume acting over the vehicle aftbody, and whether or not the plume would tend to increase or decrease the configuration's basic lateral-directional stability characteristics. Three inviscid CFD solutions were generated and analyzed to develop an understanding of this problem; full viscous (Navier-Stokes) analysis was not possible due to the large time and memory constraints associated with the problem. The first solution was generated on the inlet-closed configuration at the nominal two degrees angle-of-attack in order to offer a direct comparison with wind tunnel data. The CFD results were in good agreement with the wind tunnel data, which validated the assumption of using an inviscid analysis to capture basic lateral-directional characteristics. The second and third solutions were generated on the inlet open, unpowered and inlet open, powered configurations respectively. As shown in Fig. 10, the CFD results indicate the basic lateral-directional characteristics are essentially unchanged as a result of opening the inlet door and operating in the unpowered or powered modes. The inlet closed CFD results tended to agree well with the wind tunnel data, slightly overpredicting the magnitudes of the C_{y_β} and C_{n_β} terms, and underestimating C_{l_β} term to a small degree. This fact tends to add confidence to the conclusion that the lateral-directional characteristics are not directly affected by the expanding flow over the aftbody in the inlet open unpowered and powered configurations.

Examination of Fig. 11 indicates, however, that there is an indirect effect of the inlet open unpowered/powered operation on the airframe's lateral-directional characteristics. Recall that for the nominal Mach 7, 2 degree angle-of-attack flight condition, approximately 7 degrees of elevon deflection is required to trim the vehicle in the inlet closed configuration, while the inlet open, powered configuration trims with a near zero elevon position. The data presented in Fig. 11 indicate the fact that there is a strong dependence of both C_{l_β} and C_{n_β} on the nominal elevon position. At the nominal 2 degree angle-of-attack condition, there is a near 60% increase in the magnitude of the C_{l_β} term for elevon deflections of 7.5 degrees vs. 0 degrees, and a 17% increase in the C_{n_β} characteristic. Sideslip induced side force (C_{y_β}) remains moderately unaffected by elevon position.
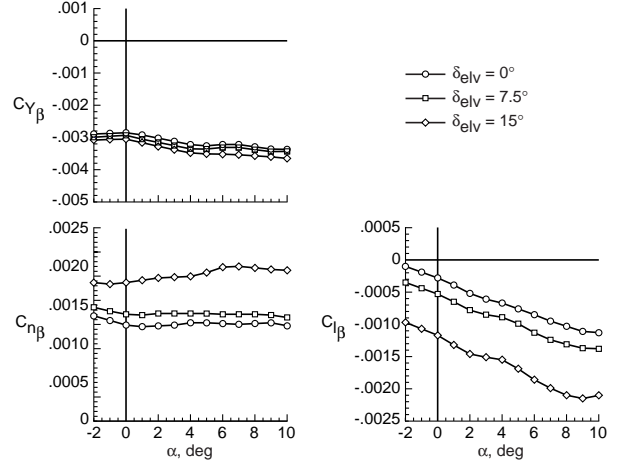

Figure 11. Effects of elevon position on the HXRV basic lateral-directional characteristics.

The effect of elevon position on the aileron control power at Mach 7 flight conditions is shown in Fig. 12. The side force, and yaw and roll moment coefficients due to linearized aileron deflections (per degree) are plotted against vehicle angle-of-attack. For the Hyper-X vehicle, aileron deflections are defined by asymmetric tail deflection about a nominal elevon (tail) position. For example, a +5 degree aileron deflection about a 0 degree elevon deflection would require a –2.5 degree left tail deflection and a +2.5 degree right tail deflection. The figures indicate a strong dependence of aileron effectiveness on the nominal elevon deflection angle. In particular, the aileron roll effectiveness is almost 70% greater about a 7.5 degree elevon deflection as opposed to a 0 degree elevon deflection.
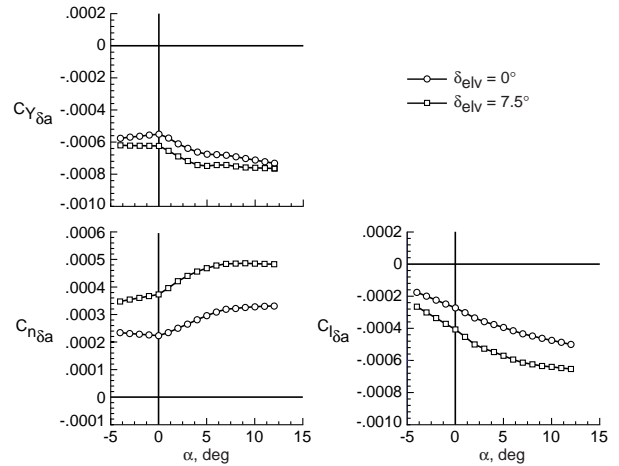

Figure 12. Effect elevon position on the HXRV aileron control effectiveness.

The fact that C_{l_β} and C_{n_β} and the aileron control power all have a strong dependency on elevon position, and elevon position is a direct function of inlet door position and engine power, indicates an indirect (though substantial) effect of engine operation on the basic airframe lateral-directional behavior and control power characteristics. This fact must be accounted for in the control law design and analysis efforts for this, and any other similar hypersonic vehicles with highly integrated propulsion systems. Control law gain scheduling may be required as a function of engine thrust levels which will directly effect the trimmed elevon position, in order to ensure that the vehicle remains in steady controlled flight during engine operations.

Finally, rudder effectiveness data at Mach 7 flight conditions, including the effects of elevon position, are shown in Fig 13. At low angles-of-attack, the rudders have a moderate amount of effectiveness, which appears to be only minimally affected by the elevon position. However, as angle-of-attack increases, the rudders tend to lose effectiveness in a rather dramatic fashion. In fact, at angles-of-attack approaching 10 degrees, the rudders are almost completely ineffective. This is due primarily to the crossflow separation occurring over the vehicle forebody which tends to bury the vertical tails and rudders in a low energy wake flow (the so-called "hypersonic shielding effect"). The design test point is at an angle-of-attack of two degrees, a condition at which the rudders do provide some degree of directional control authority. However, at a point in the flight trajectory beyond the engine test and post test tares, the vehicle must pull up to an angle-of-attack of approximately 10 degrees in order to generate enough lift to maintain altitude. At this condition, the rudders will provide little in

Figure 13. Effect of elevon position on the HXRV basic rudder control effectiveness.

the way of directional control, and the vehicle will be forced to rely on alternate methods for directional control authority and stability augmentation.

Flight Data Analysis and Reconstruction Efforts

During the flight test sequence, a series of preprogrammed aerodynamic maneuvers will be conducted in order to assess the basic aerodynamic stability and control characteristics of the vehicles at true operating flight conditions. Stability and control derivatives will be estimated by examining vehicle dynamic response to a series of preprogrammed elevator, aileron, and rudder doublets which will occur at various points in the flight trajectory. For the first Mach 7 flight, these maneuvers will be limited to the unpowered portion of flight; however, the second Mach 7 flight test profile may incorporate several maneuvers into the scramjet powered portion of the experiment, thus providing data on the propulsion system and airframe aerodynamic coupling effects under dynamic conditions. Because the engine test duration of the first flight is limited to less than 10 seconds, extensive stability information will not be obtained for the powered configuration. However, immediately prior to and following the engine test, several seconds of tare data will be taken with the inlet door in the open position. Because of the high heat loads in the combustor region flowpath, the inlet door must be returned to the closed position shortly after the engine test is complete, and remain closed for the duration of the descent. Therefore, the majority of the flight extracted stability and control information will be obtained on the inlet closed configuration. Sequential Single Surface Inputs (S^3I) for each of the elevator (pitch), rudder (yaw) and aileron (roll) surfaces will be employed, with 3-2-1-1 doublet step input profiles applied in order that time constant information can be extracted from the measured response.[11,12] These preprogrammed inputs will occur at specific intervals during most of the descent trajectory in order to capture the airframe's three axis stability and control characteristics over as much of the flight Mach envelope as possible. The inlet closed HXRV airframe drag characteristics will be captured by conducting a series of Push-Over/Pull-Up (PO/PU) angle-of-attack traversals. These maneuvers, which will also occur at specific intervals during the descent trajectory, will allow for drag polar (C_D vs. C_L or C_D vs. α) estimation at various flight Mach numbers.

In addition to the basic airframe aerodynamic stability and control parameter estimation efforts, the HXRV will be extensively instrumented with over 100 individual pressure transducers and thermocouples. Because the first priority of the Hyper-X program is to obtain data on the
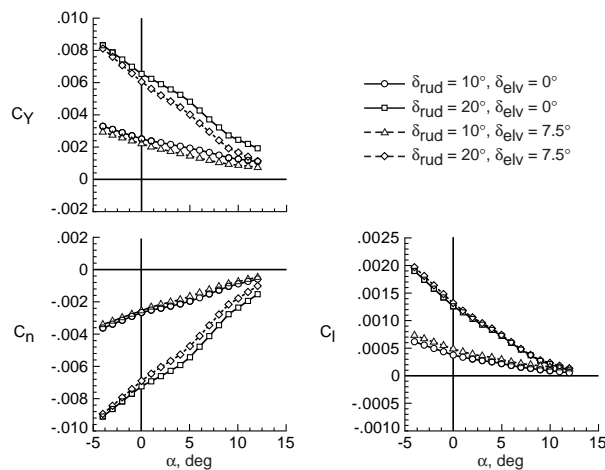
operating scramjet engines, a large percentage of the instrumentation is located within the combustor. There are, however, a significant number of pressure and temperature measurements that will be taken on the external surfaces, including the propulsion flowpath (forebody ramps and inlet, and the aftbody nozzle expansion surface) and the external airframe (forebody chines, lee/ topside, and the vehicle base). A large amount of data will collected during each flight. The nominal pressure transducer sample rate is 50Hz, and the thermocouple sample at 20Hz. For each of the three approximately 15 minute flights, the data will be taken and telemetered back to ground stations for storage and post flight analysis. The data obtained from these measurements will allow for direct comparison with the preflight CFD and analytic solutions that have been developed in support of the overall aerodynamic database effort.

Summary

An overview has been provided outlining several of the key issues surrounding airframe integrated scramjet propulsion system effects on the Hyper-X vehicle aerodynamics. Propulsion induced vehicle pitching moments and the corresponding trim drag penalties were outlined, as well as the indirect effects of the propulsion system on the lateral-directional airframe stability and control. A brief overview was provided of the experimental wind tunnel testing and CFD methods which have been, and continue to be, utilized in the development of the preflight aerodynamic database for the Hyper-X flight experiments. In order to develop the aerodynamic database to support the three Hyper-X flight test vehicles, an extensive wind tunnel test program has been executed. These wind tunnel tests have provided basic aerodynamic force and moment data over the range of anticipated flight Mach numbers for the Hyper-X flight profiles. In addition to wind tunnel test efforts, various state-of-the-art CFD codes have been and continue to be utilized to assess the effects of powered scramjet operation and the influence of the propulsion generated flowfield on the overall vehicle aerodynamics. A brief description of several of the key aerodynamic characteristics of the HXRV at or near the scramjet operation test point has also been provided. The configuration is statically stable in three axes at the design test conditions, and has adequate control power provided by the all-moving horizontal tails and the vertical tail-rudder surfaces. The airframe integrated scramjet engine operation has a substantial effect on the HXRV longitudinal trim control requirements, and an indirect effect on the lateral-directional characteristics due to the same longitudinal control deflection variations. Both the vehicle's longitudinal stability and the rudder lateral-directional control effectiveness are diminished with increased angle-of-attack beyond about eight degrees. The current schedule calls for the first Mach 7 Hyper-X flight test to fly in the spring of 2000. The data that will be collected during this first test, and the subsequent Mach 7 and 10 tests, will be utilized to validate and verify the preflight design and prediction methods, providing for continued advancement of the state-of-the-art in hypersonic vehicle integrated propulsion system-airframe aerodynamics.

References

1. Rausch, V. L., McClinton, C. R., Hicks, J. W., "NASA Scramjet Flight to Breath New Life into Hypersonics," Aerospace America, July 1997.

2. *Scramjet Propulsion (Chapter 5, Appendix B: NASA's Hyper-X Program)*, Edited by Dr. T. Curran and Dr. S.N.B. Murthy, AIAA Progress In Astronautics and Aeronautics Series, Vol. TBD, 1999.

3. Rausch, V. L., McClinton, C. R., Crawford, L., "Hyper-X: Flight Validation of Hypersonic Airbreathing Technology," ISABE Paper 97-7024, Sept. 1997.

4. Hunt, J. L., Eiswirth, E. A., "NASA's Dual-Fuel Airbreathing Hypersonic Vehicle Study," AIAA CP-96-4591, 7th International Space Planes and Hypersonics Systems & Technology Conference, Nov. 1996.

5. Bogar, T. J., Alberico, J. F., Johnson, D. B., Espinosa, A. M., Lockwood, M. K., "Dual-Fuel Lifting Body Configuration Development," AIAA CP 96-4592, 7th International Space Planes and Hypersonics Systems & Technology Conference, Nov. 1996.

6. Miller, C. G., III, "Langley Hypersonic Aerodynamic/Aerothermodynamic Testing Capabilities – Present and Future," AIAA CP-90-1376, AIAA 16th Aerodynamic Ground Testing Conference, June 1990.

7. Penaranda. F. E., and Freda, M. S., "Aeronautical Facilities Catalogue, Vol. 1 – Wind Tunnels," NASA RP-1132, Jan. 1985.

8. McClinton, C.R., Yoland, R. T., Holland, S. D., Engelund, W. C., White, J. T., and Pahle, J. W.:"Wind Tunnel Testing, Flight Scaling, and Flight Validation ith Hyper-X," AIAA 98-2866, June 1998.

9. Frendi, A., "On the CFD Support for the Hyper-X Aerodynamicd Database," AIAA 99-0855, Jan. 1999.

10. Huebner, L. D., Hodge, J. S., "Langley 8-Foot High Temperature Tunnel Testing in Support of the Hyper-X Program", Paper No. APS-CS-2H-6, Presented at the JANNAF 34th Combustion Subcommittee, Propulsion Systems Hazards Subcommittee, and Airbreathing Propulsion Subcommittee Joint Meeting, Oct. 1997.

11. Morelli, E., and Klein, V., "Optimal Input Design for Aircraft Parameter Estimation Using Dynamic Programming Principles," AIAA 90-2801, Aug. 1990.

12. Illif, K. W, Maine, R. E., and Montgomery, T. D., "Important Factors in the Maximum Likelihood Analysis of Flight Test Maneuvers," NASA TP 1459, Jan. 1979.